A CFD hybrid approach to simulate liquid-phase chemical reactors

Matteo Rizzotto [a], Federico Florit [a], Renato Rota [a], Valentina Busini [a,*]

[a] *Politecnico di Milano, Dipartimento di Chimica, Materiali e Ingegneria Chimica G. Natta, via Mancinelli 7, 20131, Milano, Italy*

**Corresponding author: valentina.busini@polimi.it +390223993186*

Highlights

- A novel CFD approach for simulate liquid reactions is proposed.
- The model can be used for any value of the kinetic and mixing characteristic times.
- Continuous reactors are analyzed as case-studies.

Abstract

Design and safety assessments of chemical reactors can be done using Reynolds Averaged Navier-Stokes (RANS) type equations. The averaging procedure of transport equations gives rise to unclosed terms, which must be properly modeled independently on the computational cell size. In particular, presence of chemical reactions leads to an additional source term in species equation. The averaged value of this term involves effects of both chemical kinetics and turbulence. Turbulence-kinetics interaction (TKI) models must be then developed in order to close species transport equations, so that Computational Fluid Dynamics (CFD) can be used to reduce the number of experiments required to design a chemical reactor.

Many TKI models have been developed in the past, mainly for gaseous systems, while liquid-phase models have been less investigated because of demanding theoretical challenges. Therefore, the purpose of this work is the development of a new TKI model for liquid phase reactions, which combines the Laminar Rate model (for kinetic controlled systems) with the Multiple Time Scales model (for turbulence controlled systems) allowing its use also when kinetic and turbulent mixing characteristic times are comparable. An analysis of the influence of the turbulence model coupled with the proposed model was carried out to identify the most

suitable turbulence model, and two different case studies were investigated to show the potentialities of the proposed approach.

Keywords: Computational fluid dynamics, MTS model, Turbulence-kinetics interaction, liquid phase reactions, Turbulent reactive flow, Micromixing

1. INTRODUCTION

In the process industry, discontinuous and continuous reactors are often used to carry out liquid phase reactions. These systems, as well as the gaseous ones, are characterized by relevant mixing phenomena (due to turbulence) and chemical transformations: mixing is the key process for which two reacting species get in contact from separate regions of the reactor. A detailed description of turbulent reactive systems is therefore of notable importance for the design and control of process equipment, especially if safety aspects are to be taken into account, such as when a runaway reaction can occur [1, 2]. In that case, not only the reactor but also the emergency quenching system involves effective and efficient mixing of a reacting mixture [3].

Turbulent mixing, along with chemical reactions and energy transfer, can be simulated using Computational Fluid Dynamics (CFD), which solves numerically the relevant mass, energy, and momentum balance equations [4]. The numerical procedure requires a discretization of the space domain through computational cells, which form the so-called mesh. Mesh elements must be small enough to capture every feature of the flow, even if the greater is the number of elements, the greater is the computational time. If the mesh dimension resolves all the details of the turbulence, the so-called Direct Numerical Simulation (DNS) can be carried out. However, DNS cannot be used to simulate cases of industrial interest, due to the huge amount of computational resources required. Therefore, equations averaged over time (Reynolds Averaged Navier Stokes, a.k.a. RANS [4]) or in space (Large Eddy Simulation, a.k.a. LES [5]) are usually solved in practice. If a chemical reaction proceeds in the system, the involved species quantities vary along space and time coordinates according also to a production or consumption rate. This term in the mass balance equation depends on both the intrinsic chemical kinetic rate, as well as on the mixing rate of the reactants. In other words, the effective production (or consumption) rate depends on both the kinetic and the turbulent characteristic time and must be computed in the RANS framework through suitable turbulence-kinetics interaction (TKI) models. This modeling is required independently on the computational cell size, as the RANS approach adopts time averaged equations regardless the mesh size. Many TKI models have been developed in the past [6, 7, 8], mainly for gaseous phase reactions (that is, for conditions characterized by the Schmidt number, Sc, equal to about one), while liquid systems (characterized by $Sc>>1$) have not been much considered. The reason is that gaseous systems are characterized by a comparable importance of momentum and mass transport. This leads to similar characteristic times of these phenomena, which simplify the

development of TKI models. Liquid systems, on the other hand, exhibit different characteristic times that must be accounted for separately with a proper model. When models developed for gaseous systems are used to represent liquid reacting systems, they generally leads to a poor description of real systems. Baldyga [9, 10] proposed a solution for liquid systems based on the spectral density functions for the concentration variance dissipation, the so-called MTS (Multiple Time Scales) model, which is supposed to work properly when Da>>1 (being Da the Damköhler number, which represents the ratio of the characteristic turbulence time to the kinetic one), that is, for turbulence controlled systems; when Da<<1 (that is, kinetic controlled systems), the average reaction rate equals the reaction rate computed at the average scalar values and the simple Laminar Rate (LR) TKI model can be used [8].

The aim of this work was to propose a new TKI approach, which combines MTS and LR methods to effectively account also for intermediate situations where neither MTS nor LR models alone are expected to work properly. The proposed approach was implemented in the commercial CFD code ANSYS Fluent 16.2 and its performance was assessed by comparison with other TKI models. Moreover, two case studies that involve a continuous reactor design were investigated to show potentialities and limits of the proposed approach.

2. MATERIAL AND METHODS

The general form of a Reynolds averaged transport equation for a generic scalar ϕ, assuming isotropic conditions, is [4]:

$$\frac{\partial(\rho\phi)}{\partial t} + \nabla(\rho\phi\boldsymbol{v}) = \nabla\left(\Gamma_\phi \nabla\phi\right) + S_\phi \quad \#(1)$$

where ρ is the fluid density, $\boldsymbol{v}$ the velocity vector, Γ_ϕ is the effective scalar diffusivity and S_ϕ is the scalar source term. These last two quantities must be computed through a suitable model since both include the influence of turbulence. Effective diffusivity is generally expressed as sum of a molecular term (density times molecular diffusivity for species, thermal conductivity for energy, and dynamic viscosity for momentum transport) and a turbulent term.

In the frame of RANS models, the turbulent viscosity is calculated with specific models, which introduce further transported variables. Among these, the well-known $\kappa - \epsilon$ model [4, 5, 11] uses the turbulent kinetic energy, κ, and the turbulent dissipation rate, ϵ, as additional transported variables., while the $\kappa - \omega$ model [4, 5] uses the specific turbulent dissipation rate, ω, instead of the turbulent dissipation rate ϵ. The $\kappa - \omega$ SST model [4] uses a $\kappa - \omega$ model in the inner parts of the boundary layer, allowing the model to be used all the way down to the wall through the viscous sub-layer: this actually makes it a low Reynolds (Low Re) model. The SST formulation of the $\kappa - \omega$ model switches to a $\kappa - \epsilon$ model in the free-stream, therefore avoiding some known problems of the $\kappa - \omega$ model (for example, it is too much sensitive to the turbulent properties of the inlet free-stream).

Also, the source terms require additional models to compute them. In the species transport equation, these models are called TKI models. The time averaged species transport equation can be deduced from the general equation (1), whereas $\phi = \omega_k$, as:

$$\frac{\partial(\rho\omega_k)}{\partial t} + \nabla(\rho \boldsymbol{v}\omega_k) = -\nabla\left(\rho\mathfrak{D}_{eff}\nabla\omega_k\right) + \overline{\dot{\Omega}_k} \qquad k = 1 \dots NC \ \#(2)$$

where ω_k is the species k mass fraction, $\mathfrak{D}_{eff} = \mathfrak{D} + \mathfrak{D}_t$ is the effective diffusivity ($\mathfrak{D}_t = \frac{\mu_t}{\rho \cdot Sc_t}$ represents the turbulent diffusivity), NC is the number of species, and $\overline{\dot{\Omega}_k}$ is the average species production (or consumption, when negative) rate, that can be computed as the product of an always positive scalar (the reaction rate) times the stoichiometric coefficient of the k-th species assumed positive for products and negative for reactants. Given the high non-linearity of $\dot{\Omega}_k$, its average value differs from the value computed using the averaged properties. A model for computing this term is then required to properly close the species transport equation. The averaged reaction rate will then depend on the fluid dynamics of the system, and consequently from the chosen turbulence model. The different turbulence models used in the simulations discussed in the following are reported in the caption of the corresponding figures.

2.1. TKI models

In the following, the various TKI models from the literature that have been used for the calculation of the average reaction rate are briefly presented. The novel TKI approach for liquid phase reactions is also proposed.

2.1.1 Laminar Rate model (LR)

For an irreversible single-step reaction $\nu_A A + \nu_B B \rightarrow \nu_C C + \nu_D D$, with negligible pressure effects (as in liquid phase reactions), the production (or consumption) rate can be computed through an Arrhenius rate constant times a power law using the average values of both temperature and species concentration [8]:

$$\overline{\dot{\Omega}_k} = \nu_k \mathcal{K}_0 \exp\left(-\frac{E_a}{RT}\right) MW_k \prod_{i=1}^{NC} c_i^{\alpha_i} \quad \#(3)$$

where ν_k is the stoichiometric coefficient of species k, $\mathcal{K}_0$ is the Arrhenius pre-exponential factor, E_a is the activation energy, R is the universal gas constant, T is the time averaged absolute temperature, MW_k is the molecular weight of species k, c_i is the time averaged molar concentration of species i, and α_i is the reaction order of species i. As it can be noted, this model does not include the effects related to turbulence. For this reason, it is usually called Laminar Rate model. As a strength, the model is suitable for well mixed systems (Da<<1), where the chemical reaction is dominant over scalar transport in determining the overall consumption or production rate.

Equation (3) represents the generic form of a massive production (or consumption) rate for a transformation limited by chemical reactions. The molar reaction rate for an isothermal system can be written as $r = \mathcal{K} \prod_{i=1}^{NC} c_i^{\alpha_i}$, where $\mathcal{K} = \mathcal{K}_0 \exp\left(-\frac{E_a}{RT}\right)$ at a given temperature, so $\overline{\dot{\Omega}_k} = \nu_k r MW_k$. The particular expression of r will be reported in every paragraph of chapter 3, making explicit the values of $\mathcal{K}$ and α_i used.

2.1.2 Eddy Dissipation Model (EDM)

Fast irreversible single-step reactions are limited by the mixing rate of the reactants and not by the intrinsic chemical kinetics when Da>>1. Considering an irreversible single-step reaction $A + \nu_B B \rightarrow \nu_C C$, a turbulence-limited reaction rate can be computed as [7]:

$$\overline{\dot{\Omega}_k} = \nu_k \mathcal{A} \rho \frac{\epsilon}{\kappa} \min\left(\omega_A, \frac{\omega_B}{s}, \mathcal{B}\frac{\omega_C}{1+s}\right) \quad \#(4)$$

where $s = \nu_B \, MW_B/MW_A$, $\mathcal{A}$ is a numerical constant equal to 4 in the case of gases [8], and $\mathcal{B}$ is another constant, whose value has been chosen arbitrarily high in order to avoid product limited reaction rates.

2.1.3 Scalar Dissipation Theory model (EDM-SDT)

Fox [12,13,14] has proposed a modification to the EDM to be used with fluids having a Schmidt number greater than 1 (that is, liquids), and has derived the scalar dissipation rate divided by its variance, equivalent to ϵ/κ in equation (4), as:

$$\frac{\epsilon}{\kappa} = \frac{2 + Sc^{-1}}{2}\left(\frac{3\langle u'^2\rangle}{4\epsilon} + \frac{1}{2}\ln(Sc)\left(\frac{\nu}{\epsilon}\right)^{0.5}\right)^{-1} \quad \#(5)$$

where $\langle u'^2\rangle$ is the mean value of velocity fluctuations, and ν is the kinematic viscosity. In this model $\mathcal{A}$ and $\mathcal{B}$ values are the same as in the EDM.

2.1.4 Multiple Time Scale model (MTS)

Liquid reactions (Sc>>1) are mainly influenced by concentration gradients [8] rather than temperature gradients. A measure of the variance of local concentration is therefore an index of unmixedness and strongly affects reaction rates. In this context, a spectral density function of concentration distribution becomes useful and can be divided into three ranges [9]:

1) inertial-convective;
2) viscous-convective;
3) viscous-diffusive.

It is assumed that concentration variances (σ_i^2, where $i = 1, 2, 3$ refers to the subrange) in these subranges are transported as generic scalars, together with the so-called mixture fraction f. The mixture fraction is a conserved scalar describing all possible mixture of reagents and it can vary between 0 and 1; therefore, it is a measure of unmixedness.

Their transport equations are [10, 15, 16]

$$\rho \frac{D\sigma_i^2}{Dt} = \nabla\left(\rho \mathfrak{D}_{eff} \nabla \sigma_i^2\right) + \dot{\Omega}_{\sigma_i^2}^{prod} - \dot{\Omega}_{\sigma_i^2}^{diss} \quad i = 1, 2, 3 \; \#(6)$$

$$\rho \frac{Df}{Dt} = \nabla(\rho \mathfrak{D} \nabla f) \#(7)$$

since dissipation can be seen as an energy cascade, σ_1^2 production term ($\dot{\Omega}_{\sigma_1^2}^{prod}$) comes from unmixedness, σ_1^2 dissipation term ($\dot{\Omega}_{\sigma_1^2}^{diss}$) is equal to σ_2^2 production term ($\dot{\Omega}_{\sigma_2^2}^{prod}$), and σ_2^2 dissipation term ($\dot{\Omega}_{\sigma_2^2}^{diss}$) is equal to σ_3^2 production term ($\dot{\Omega}_{\sigma_3^2}^{prod}$).

By averaging in time the transport equation for f and analyzing its variance transport equation, it is possible to derive the following relation for the production rate of σ_1^2 [10, 15, 16]:

$$\dot{\Omega}_{\sigma_1^2}^{prod} = 2 \frac{\mu_t}{Sc_t} \|\nabla f\|^2 = 2\rho \mathfrak{D}_t \|\nabla f\|^2 \#(8)$$

where μ_t is the turbulent dynamic viscosity, and Sc_t is the turbulent Schmidt number.

The inertial-convective subrange ranges from the macroscale (the largest scale of turbulence) down to the Kolmogorov scale. The viscosity does not influence the flow (inertial flow) and there is no influence of molecular diffusion (convective mass transfer). In this subrange there is neither creation nor destruction of both kinetic energy and concentration variance, but some parts of the fluid are deformed leading to a scale reduction (thinning).

Introducing the dissipation decay time $\tau = \frac{\kappa}{\epsilon}$, it is possible to model the variance dissipation rate as [10, 15, 16]

$$\dot{\Omega}_{\sigma_1^2}^{diss} = \rho \frac{\sigma_1^2}{\tau} = \rho \mathcal{R} \frac{\epsilon}{\kappa} \sigma_1^2 = \dot{\Omega}_{\sigma_2^2}^{prod} \#(9)$$

where $\mathcal{R} = 2$ represents the timescales ratio for the decay of velocity fluctuations to concentration ones.

The viscous-convective subrange ranges from the Kolmogorov scale down to the Batchelor scale [17]. Laminar stresses further reduce the scale with almost no influence of molecular diffusion. Using the same approach as for the inertial-viscous subrange, decay time is used in order to obtain [10, 15, 16]

$$\dot{\Omega}_{\sigma_2^2}^{diss} = \rho E \sigma_2^2 = \rho 0.0578 \left(\frac{\epsilon}{\nu}\right)^{\frac{1}{2}} \sigma_2^2 = \dot{\Omega}_{\sigma_3^2}^{prod} \#(10)$$

where *E* is the engulfment parameter.

The viscous-diffusive subrange is characterized by an equal relevance of laminar stresses and diffusion where the eddies are smaller than the Batchelor scale. Using Baldyga's simplification [10], first order kinetics for variance in the viscous-diffusive subrange can be written as

$$\dot{\Omega}_{\sigma_3^2}^{diss} \approx \rho G \sigma_3^2 = \rho \left(0.303 + \frac{17051}{Sc}\right) \cdot E \sigma_3^2 \#(11)$$

where *G* is a molecular diffusion parameter.

From the values of the different variances an overall variance $\sigma_s^2 = \sigma_1^2 + \sigma_2^2 + \sigma_3^2$ can be computed and used to estimate the turbulence characteristic time [10]

$$\tau_T = \frac{\sigma_s^2}{G \sigma_3^2} \#(12)$$

In reactive turbulent system involving fast irreversible single-step reactions rates (Da>>1), the production (or consumption) rate is determined by the turbulence characteristic time. Considering the following general reaction

$$A + \nu_B B \rightarrow \nu_C C \ \#(13)$$

and defining $s = \frac{\nu_B MW_B}{MW_A}$, the final expression of the production (or consumption) rate can be found as [10, 15, 16]:

$$\bar{\dot{\Omega}}_k = \mathcal{A} \rho \frac{G \sigma_3^2}{\sigma_s^2} \min\left(\omega_A, \frac{\omega_B}{s}\right) \#(14)$$

where $\mathcal{A}$ is a constant equal to 1 in the case of liquid reactions [15, 16]. As expected, there is no influence of kinetics in this equation, since turbulent transport controls the overall production (or consumption) rate. In other words, reactants immediately get consumed when they get in contact. In the frame of TKI models for

combustion systems, this approach is called “mixed-is-burned” approach. Equation (14) represents the Multiple Time-Scales (MTS) model.

2.1.5 Proposed hybrid approach (LR – MTS)

Considering a generic second order reaction, the characteristic reaction rate can be represented by the general relation

$$\bar{R} = \mathcal{K}\bar{c}^2 \#(15)$$

Therefore, a kinetic characteristic time can be estimated as:

$$\tau_R = (\mathcal{K}\bar{c})^{-1} \#(16)$$

Comparing the turbulence characteristic time (12) with the kinetic one (16), the local value of the Damköhler number can be computed in each cell of the computational domain as [18]:

$$Da = \frac{\tau_T}{\tau_R} \#(17)$$

When in a computational cell Da>>1 the controlling step is transport (mixing limited) and MTS model can be used, while when Da<<1 chemical reaction is the controlling step (reaction limited) and LR model can be used. However, when the two characteristic times are comparable ($Da \approx 1$), neither MTS nor LR can be used to estimate the production (or consumption) rate.

As usually done for gas-phase reactions by the so-called LR-EDM approach [8], in the transition region from Da<<1 to Da>>1 a hybrid approach (in the following referred to as LR-MTS) could be introduced. This new approach computes the local production (or consumption) rate as the smallest between the values computed using the MTS and LR models:

$$\bar{\dot{\Omega}}_k = \nu_k \min\left(\mathcal{K} M W_k \prod_{i=1}^{NC} c_i^{\alpha_i} \, , \mathcal{A}\rho \frac{G\sigma_3^2}{\sigma_s^2} \min\left(\omega_A, \frac{\omega_B}{s}\right) \right) \#(18)$$

In other words, the LR-MTS approach requires computing in each computational cell two values of the production (or consumption) rate using both the LR and the MTS formulations (i.e., using the previously discussed Equations (3) and (14), respectively). Once these two values are computed in all the computational cells, in each cell the smallest one is used to compute the local production (or consumption) rate. This approach, following the same lines as the LR-EDM approach used for gas-phase reactions [8], arises from a

comparison of the characteristic times (which are inversely proportional to the rates) of the two key physical processes that can determine the production (or consumption) rate, namely: mixing and chemical kinetics. When mixing and reaction characteristic times are comparable the overall rate can be calculated with both models interchangeably; while, when one characteristic time is greater than the other one, it should be chosen as the rate determining one. This approach was implemented in Fluent through user-defined functions (UDF) and user-defined scalars (UDS), which allow for performing in each computational cell the aforementioned comparison.

3. Results and discussion

3.1. Sensitivity analysis

The proposed hybrid approach requires computing in each cell the production (or consumption) rate using both the LR model (3) and the MTS model (14). While the LR model does not involve any turbulence-related quantity, the MTS model involves the turbulent dynamic viscosity value, which in turn is computed from the turbulence model used. Therefore, it is expected that the results of the MTS model (and consequently of the LR-MTS model) could depend on the turbulence model selected. In the following, the performance of the LR-MTS model is compared at first with both some experimental values and the predictions of other TKI models showing, in conditions characterized by Da>>1, the superior performance of the proposed model. Moreover, the influence of the selected turbulence model on the LR-MTS model performance is also investigated.

The kinetic parameters used for the simulations are reported in the following sections; the values of the constants involved in the various models have been set equal to the default values proposed in the commercial CFD code ANSYS Fluent 16.2.

3.1.1. Obstructed reactor

The first set of experimental data were measured in a steady-state isothermal square section reactor equipped with a central obstruction [19], located at the center of the channel, as sketched in Figure 1. An acid solution A (acetic acid) has been injected from one side of the obstruction, while a basic solution B (ammonium hydroxide) has been fed from the other side, leading to a neutralization reaction into the reactor [20, 21]:

$$CH_3COOH + NH_4OH \rightarrow CH_3COONH_4 + H_2O$$

$$r = \mathcal{K} c_A c_B \quad \mathcal{K} \approx 1E11\, m^3 kmol^{-1} s^{-1} \#(19)$$

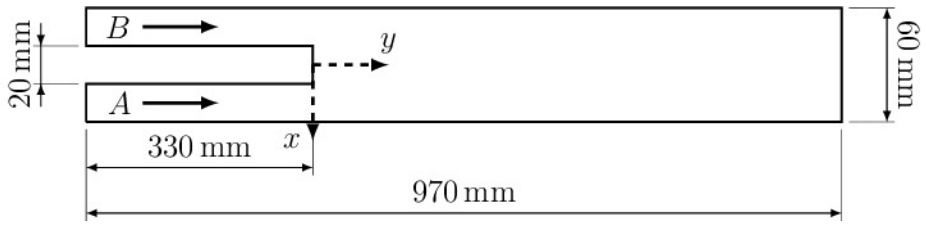

Figure 1 Obstructed reactor geometry. Cartesian axes are dashed and represent the origin of the coordinates system.

This reactor was simulated using the boundary conditions reported in Table 1. After a mesh independence analysis, the number of hexahedral cells used for the computations was set equal to about 900,000.

Inlet A	$\omega_A = 6E-4$ $v_A = 0.170 \frac{m}{s} \quad (Re = 6800)$ $v_A = 0.085 \frac{m}{s} \quad (Re = 5100)$ $f = 1$ $\sigma_1^2 = \sigma_2^2 = \sigma_3^2 = 0$
Inlet B	$\omega_A = 3.5E-4$ $v_B = 0.170 \frac{m}{s} \quad (Re = 6800\ and\ 5100)$ $f = 0$ $\sigma_1^2 = \sigma_2^2 = \sigma_3^2 = 0$
Outlet	$Mixture\ fraction\ flux = 0$ $Variances\ flux = 0$
Wall	No slip condition

Table 1 Boundary conditions used for simulating the obstructed reactor sketched in Figure 1

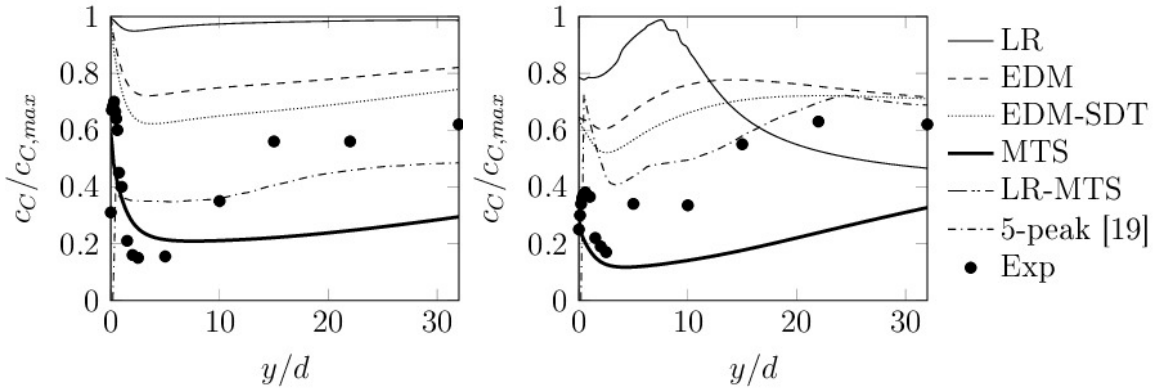

Figure 2 Obstructed reactor product dimensionless concentration distribution along the axial coordinate computed using the $\kappa - \epsilon$ model compared with experimental data in [19] for v_A/v_B=1 on the left and for v_A/v_B=0.5 on the right. MTS and LR-MTS results overlap. The model results reported by Hjertager Osenbroch et al. [19] are also shown for comparison.

Simulation results obtained using the turbulence $\kappa - \epsilon$ model are reported in Figure 2 for different TKI models together with the experimental data. In particular, LR model (3), EDM model [6], EDM-SDT model [12, 13, 14], MTS model (14), and LR-MTS model (18) were compared (note that MTS model and LR-MTS model predictions are coincident, being in these conditions Da>>1 in all the computation cells). As expected, no model but MTS and LR-MTS have a reasonable agreement with the experimental data in the first part of the reactor (that is, in the proximity of the obstruction), where experimental data show a stagnation of product close to the obstruction, probably due to recirculation. A stagnant region is predicted by all models, but LR, EDM, and EDM-SDT models overpredict the reaction rate, resulting in an overestimation of product concentration in the stagnation region. Increasing the axial coordinate, the MTS and LR-MTS models become less accurate, predicting a lower product concentration. This behavior is probably due to a too low predicted reaction rate or to an excessive dilution effect of the model.

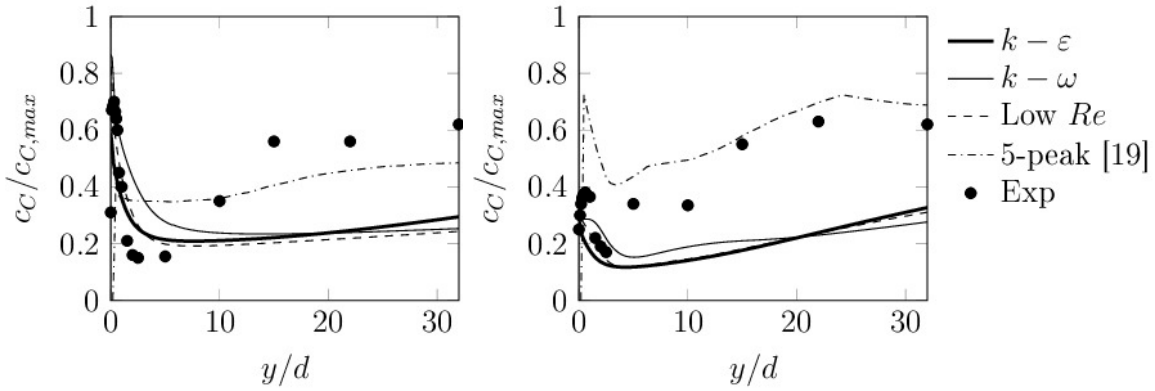

Figure 3 Obstructed reactor product dimensionless concentration distribution along the reactor axis predicted using the MTS model (or equivalently the LR-MTS model) together with different turbulence models compared with experimental data in [19] for v_A/v_B=1 on the left and for v_A/v_B=0.5 on the right. The model results reported by Hjertager Osenbroch et al. [19] are also shown for comparison.

In Figure 3 the results computed using different turbulence models together with the MTS model (or LR-MTS: the two models give the same results) are shown. We can see that there are no large differences among the investigated turbulence models.

For the sake of completeness, also the modeling results present in [19] were reported in the figure, even if they were obtained with a completely different approach (e.g., a 5-peak pdf one). This pdf approach is based on statistical considerations on the turbulence structure, and is generally much more computationally expensive. As it can be seen from the figure, also this completely different (and much more complex) model cannot reproduce the whole data set.

3.1.2. First tubular reactor

The second set of experimental data investigated has been carried out in the steady-state isothermal tubular reactor sketched in Figure 4 [22]. It has been equipped with a capillary inlet, concentric to the larger reactor pipe.

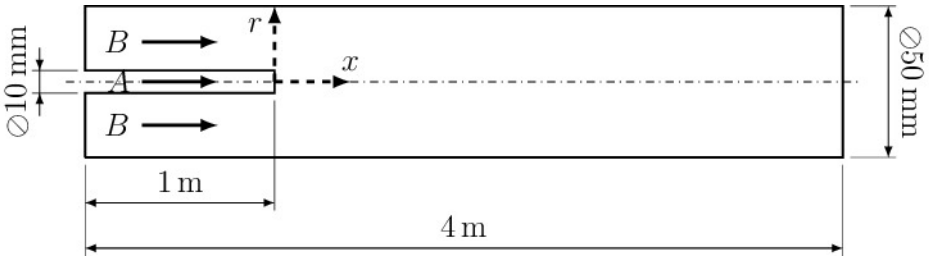

Figure 4 First tubular reactor geometry. Cartesian axes are dashed and represent the origin of the coordinates system.

An acid solution A (hydrochloric acid) has been injected from the capillary, while an alkaline solution B (sodium hydroxide) has been fed through the circular corona between the capillary and the wall, leading to a neutralization reaction in the reactor [23]:

$$HCl + NaOH \rightarrow NaCl + H_2O$$

$$r = \mathcal{K} c_A c_B \quad \mathcal{K} = 1.692E11\, m^3 kmol^{-1} s^{-1} \#(20)$$

In Table 2 the boundary conditions used for simulating this reactor are reported.

Inlet A	$\omega_A = 3.6E-2$ $v_A = 1.5 \frac{m}{s}$ $f = 1$ $\sigma_1^2 = \sigma_2^2 = \sigma_3^2 = 0$
Inlet B	$\omega_B = 4E-2$ $v_B = 0.3125 \frac{m}{s}$ $f = 0$ $\sigma_1^2 = \sigma_2^2 = \sigma_3^2 = 0$
Outlet	$Mixture\ fraction\ flux = 0$ $Variances\ flux = 0$
Wall	No slip condition

Table 2 Boundary conditions used for simulating the tubular reactor sketched in Figure 4

In this case, it was possible to use the symmetry boundary condition taking advantage of the axial symmetry of the reactor. This greatly reduces the number of cells required: after a mesh independence analysis, the number of cells used for all the computations was equal to about 50,000.

Simulation results obtained using the $\kappa - \epsilon$ turbulence model for the concentration distribution along the axis are reported in Figure 5.

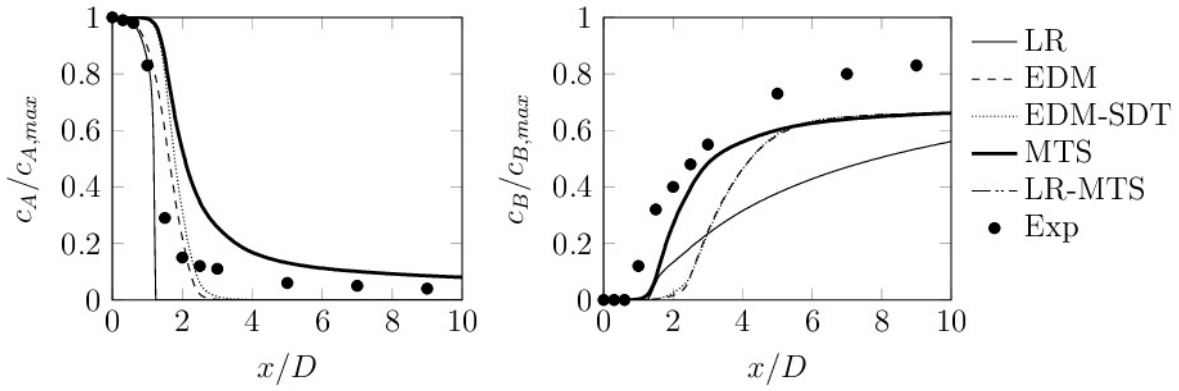

Figure 5 Tubular reactor reagents dimensionless concentration distribution along the reactor axis using the $\kappa - \epsilon$ turbulence model compared with experimental data in [22]. Acid concentration on the left, base concentration on the right. MTS and LR-MTS results overlap.

As expected (since the reaction is very fast), LR model predicts a sudden consumption of acid and base. The base concentration then increases along the axis solely due to dilution effect. Concentration values calculated using EDM and EDM-SDT models are substantially the same, while MTS model follows the experimental trend quite reasonably in the first part of the reactor. Again, MTS and LR-MTS model predictions coincide as the intrinsic chemical reaction is very fast. Dilution effects are dominating in the second part, as can be noted by observing the overestimation of acid concentration and the underestimation of base concentration. This means that the reaction region length is overestimated. A complete consumption of the acid reagent is correctly not predicted by the MTS and LR-MTS models, contrary to the other TKI models which force concentration gradients to be dissipated quickly. Comparing experimental data and model results for the radial velocity profile along the reactor shown in Figure 6, it can be concluded that the previously discussed differences among measured species concentration and model predictions should be ascribed to the TKI model.

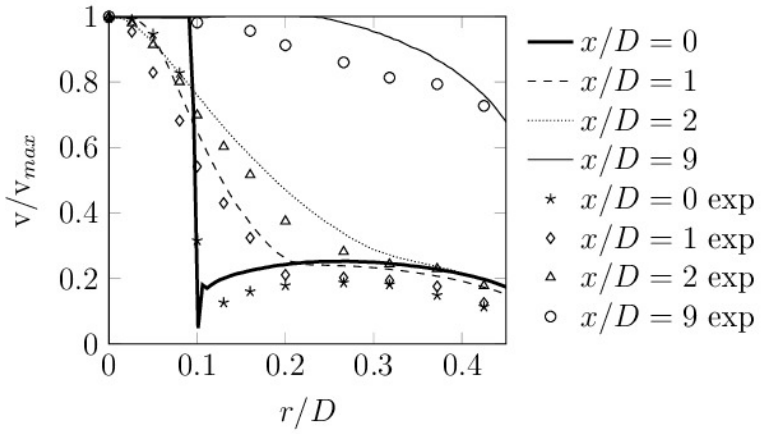

Figure 6 Tubular reactor dimensionless velocity distributions at different axial coordinates along the radial direction computed using MTS (or equivalently the LR-MTS model) with $\kappa - \epsilon$ model compared to experimental data in [22].

This is confirmed by the turbulence model analysis, whose results are shown in Figure 7. We can see that the $\kappa - \epsilon$ model and the low Re model lead to very similar results, while the $\kappa - \omega$ model predicts initial data slightly better, while it has the same behavior in the second part of the reactor.

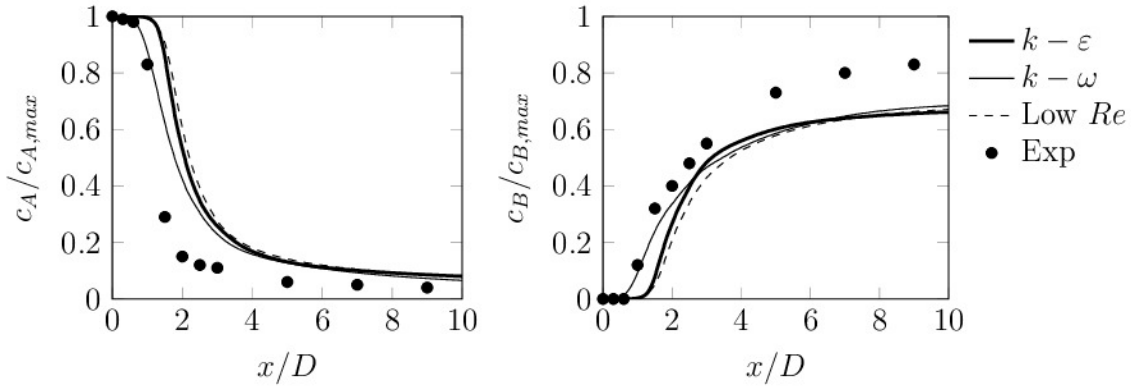

Figure 7 Tubular reactor reagents dimensionless concentration distribution along the axis computed using MTS model (or equivalently the LR-MTS model) together with different turbulence models compared to experimental data in [22].

3.1.3. Second tubular reactor

The third set of experimental data investigated has been carried out in the steady-state isothermal tubular reactor sketched in Figure 8 [24].

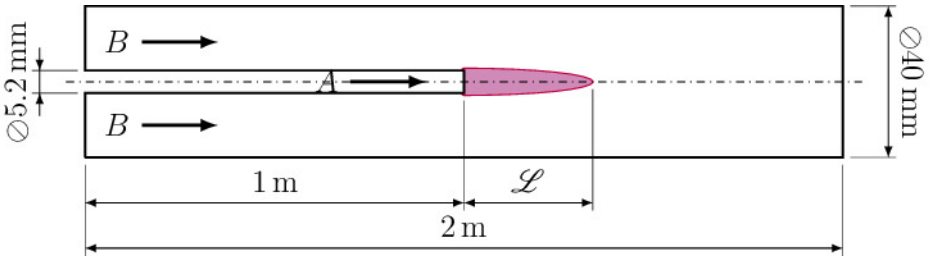

Figure 8 Second tubular reactor geometry

An alkaline solution A (sodium hydroxide) has been injected from the capillary (concentric to the larger reactor tube), while an acid solution B (hydrochloric acid) has been fed to the circular corona between the capillary and the reactor wall, leading to a neutralization reaction [23]:

$$HCl + NaOH \rightarrow NaCl + H_2O$$

$$r = \mathcal{K} c_A c_B \quad \mathcal{K} = 1.692E11\, m^3 kmol^{-1} s^{-1} \#(21)$$

This reactor configuration was simulated using the boundary conditions reported in Table 3.

Inlet A	$\omega_A = 4E-4$ $v_A = 0.325 \frac{m}{s} \quad (Re = 13000)$ $v_A = 0.5 \frac{m}{s} \quad (Re = 20000)$ $v_A = 0.625 \frac{m}{s} \quad (Re = 25000)$ $f = 1$ $\sigma_1^2 = \sigma_2^2 = \sigma_3^2 = 0$
Inlet B	$\omega_B = 5.47E-4$ $v_B = 0.325 \frac{m}{s} \quad (Re = 13000)$ $v_B = 0.5 \frac{m}{s} \quad (Re = 20000)$ $v_B = 0.625 \frac{m}{s} \quad (Re = 25000)$ $f = 0$ $\sigma_1^2 = \sigma_2^2 = \sigma_3^2 = 0$
Outlet	$Mixture\ fraction\ flux = 0$

	$Variances\ flux = 0$
Wall	No slip condition

Table 3 Boundary conditions used for simulating the tubular reactor sketched in Figure 8

Also in this case, it was possible to use the symmetry boundary condition, therefore reducing the number of cells required: after a mesh independence analysis, the number of cells used in all the computations was equal to about 70,000.

Experimentally, a plume emerged from the capillary, whose length, $\mathcal{L}$, was estimated as the maximum axial coordinate for a 95% sodium hydroxide conversion. The results obtained using different TKI models coupled to the $\kappa - \epsilon$ turbulence model are summarized in Figure 9, in terms of parity plot for the experiments considered.

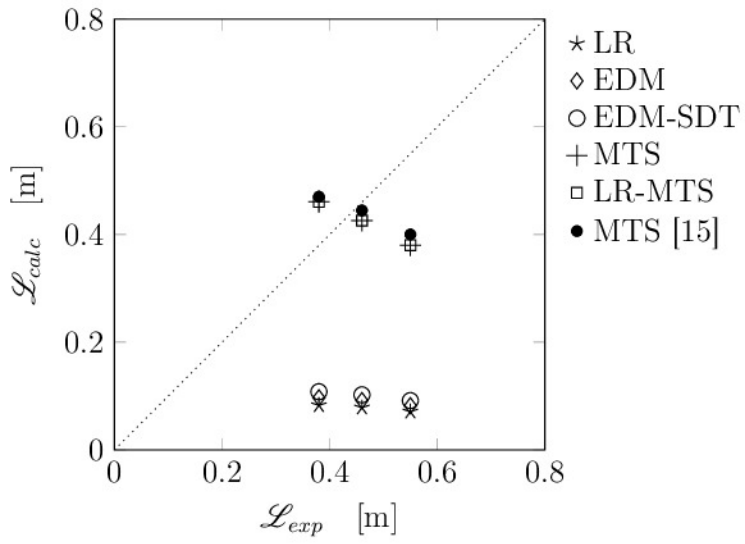

Figure 9 Second tubular reactor plume length computed using various TKI models with $\kappa - \epsilon$ model vs. the experimental values in [24]. The model results reported by Hjertager et al. [15] are also shown for comparison.

As expected MTS and LR-MTS models predict the same results, and also in this case each model but these two is unable to predict a reasonable value for the reaction region. It can be noted that MTS and LR-MTS model predictions are in line with literature results [15]. However, in this case different turbulence model seem to affect the predicted plume length, as shown in Figure 10.

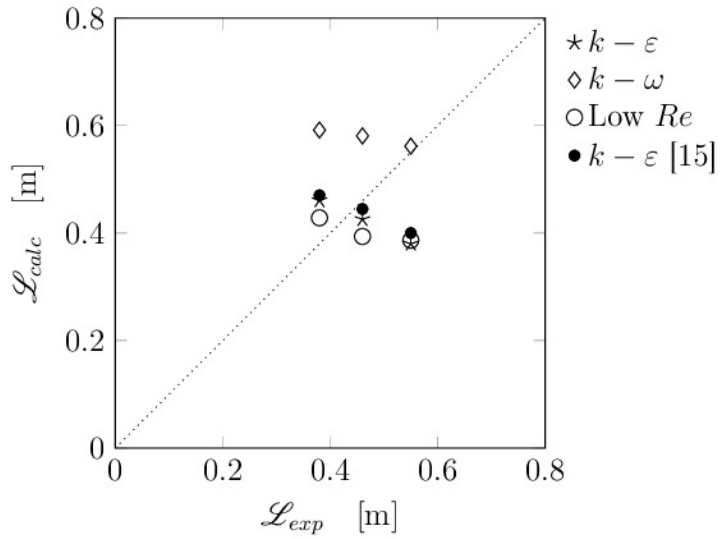

Figure 10 Second tubular reactor plume length computed using MTS model together with different turbulence models vs. the experimental values in [24]. The model results reported by Hjertager et al. [15] are also shown for comparison.

In particular, $\kappa-\omega$ turbulence model predicts values slightly different from those of the $\kappa-\epsilon$ and Low Re models, which lead to similar results.

For the sake of completeness, also the modeling results reported in [15] were shown in the figures. As expected, since the model used in [15] was the $\kappa-\epsilon$ coupled with MTS, the literature results are almost superimposed with the results we found using the same approach, therefore representing an independent cross validation of the model results reported in this paper.

3.2. Case studies

In the following, an assessment of two qualitative behaviors that should characterize the proposed approach is investigated. In particular, since the reaction rate is evaluated in each cell of the computational domain as the smallest between the LR and MTS values, the solution obtained using the hybrid LR-MTS model should lead always to conversion values lower or equal to that predicted by the LR and MTS model. Moreover, for Da<<1 or Da>>1 the LR-MTS model must provide results equal to those of the LR or MTS model, respectively.

For the analysis of these two points, two distinct case studies were investigated. The former is a tubular reactor with multiple intermediate feeds, the latter is a tubular reactor equipped with a static mixer. Also in

this case, apart from the kinetic parameters (whose values are reported in the following sections), for all the values of the constants involved in the various models the default values proposed in the commercial CFD code ANSYS Fluent 16.2 were used.

3.2.1. Tubular reactor with intermediate feeds

The first case study involves an isothermal tubular reactor with intermediate feeds with two concentric tubes positioned along the tube axis, as shown in Figure 11.

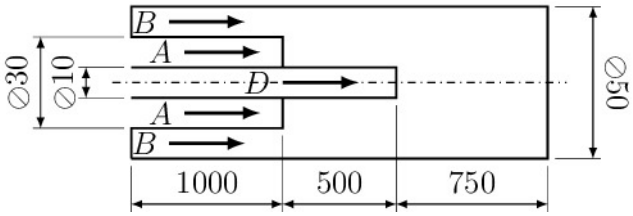

Figure 11 Tubular reactor with intermediate feeds geometry.

The process involved is supposed to produce a valuable species E through a series of two consecutive reactions

$$A + B \rightarrow C \quad r_1 = \mathcal{K}_1 c_A c_B$$

$$C + D \rightarrow E \quad r_2 = \mathcal{K}_2 c_C c_D \#(22)$$

where $\mathcal{K}_1 = 30\, m^3 kmol^{-1} s^{-1}$ and $\mathcal{K}_2 = 1E11\, m^3 kmol^{-1} s^{-1}$.

A was fed from the largest inner tube, D from the smallest one and B from the outer corona. All reagents were fed in aqueous diluted solutions in stoichiometric quantities. As two reactions are present, two mixture fractions were defined along with appropriate variances for MTS and LR-MTS models: f_1 is the mixture fraction describing all possible mixtures of A and B, and f_2 is the mixture fraction describing all possible mixtures of C and D.

Boundary conditions used to simulate such a tubular reactor are reported in Table 4.

Inlet A	$\omega_A = 4E-3$ $v_A = 0.6\frac{m}{s}$ $f_1 = 1$ $f_2 = 0$ $\sigma_{11}^2 = \sigma_{21}^2 = \sigma_{31}^2 = 0$ $\sigma_{12}^2 = \sigma_{22}^2 = \sigma_{32}^2 = 0$
Inlet B	$\omega_B = 4E-3$ $v_B = 0.3\frac{m}{s}$ $f_1 = 0$ $f_2 = 0$ $\sigma_{11}^2 = \sigma_{21}^2 = \sigma_{31}^2 = 0$ $\sigma_{12}^2 = \sigma_{22}^2 = \sigma_{32}^2 = 0$
Inlet D	$\omega_B = 2.4E-2$ $v_B = 0.8\frac{m}{s}$ $f_1 = 0$ $f_2 = 1$ $\sigma_{11}^2 = \sigma_{21}^2 = \sigma_{31}^2 = 0$ $\sigma_{12}^2 = \sigma_{22}^2 = \sigma_{32}^2 = 0$
Outlet	$Mixture\ fraction\ flux = 0$ $Variances\ flux = 0$
Wall	No slip condition

Table 4 Boundary conditions used for simulating the tubular reactor with intermediate feeds

Also in this case, it was possible to use the symmetry boundary condition thanks to the axial symmetry of the reactor. After a mesh independence analysis, the number of cells used in all the computations was equal to about 370,000.

Yield was used as a target parameter to compare the performance of the various TKI models, and it is defined as

$$\eta_E = \frac{\dot{n}_E}{\dot{n}_D^0} = \frac{\int_{\mathcal{A}} c_E \boldsymbol{v} \cdot \underline{n} dA}{c_D^0 \mathcal{A}_D v_D^0} \#(23)$$

where $\underline{n}$ is the normal of the cross section $\mathcal{A}$.

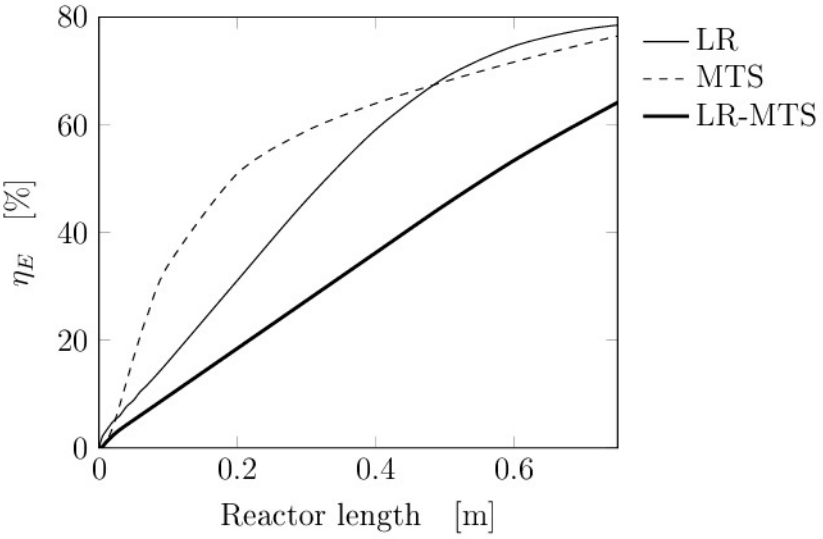

Figure 12 Valuable product yield as a function of reactor length according to different TKI models coupled with the $\kappa - \epsilon$ turbulence model .

In Figure 12 the model results obtained using the LR, MTS, and LR-MTS TKI models are reported in terms of yield. Quite a large difference between the results obtained using the various analyzed models was found. However, we can see that LR-MTS correctly predicts lower yield values, as expected being the reaction rate always lower than that of both LR and MTS models, therefore limiting conversion and yield.

The different behavior of these models can be evidenced by the predicted reaction rate profiles, as shown in Figure 13, where the hybrid nature of the LR-MTS model is quite evident.

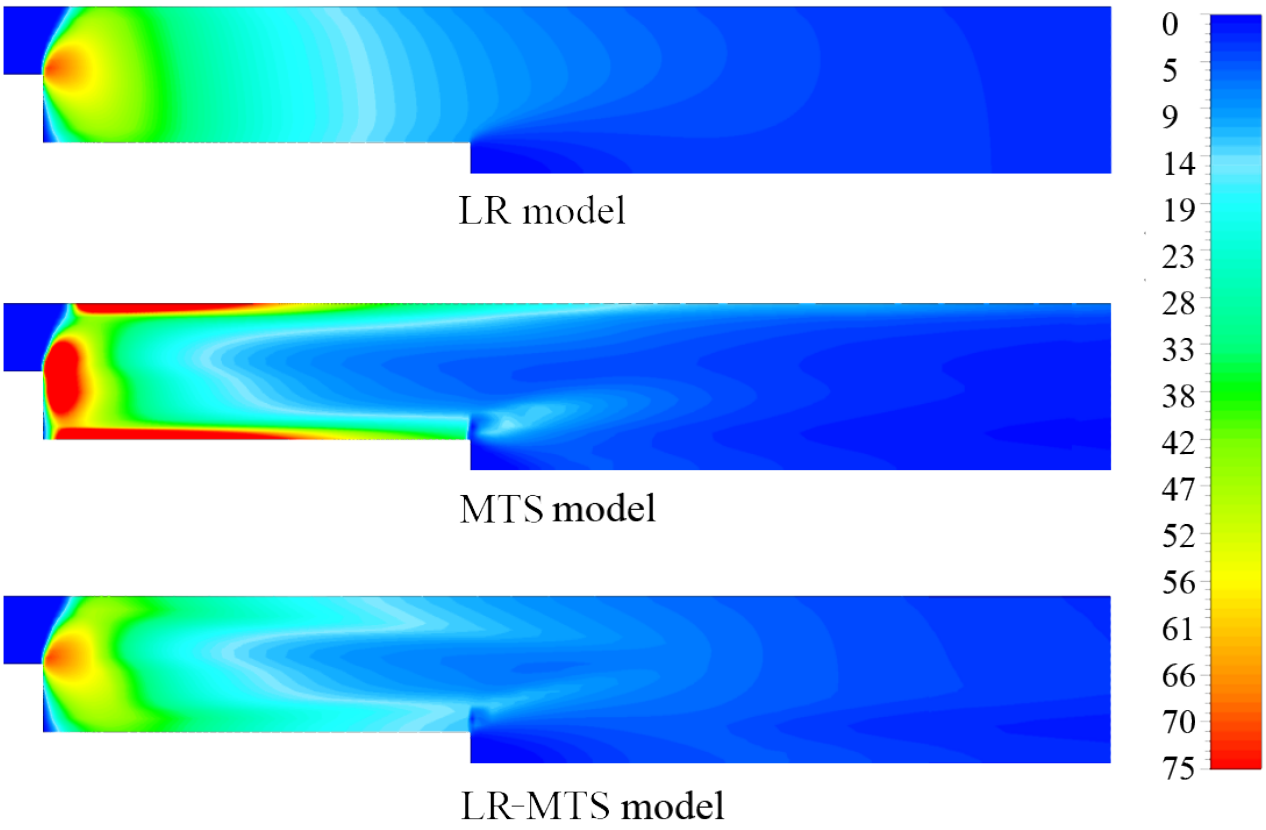

Figure 13 Reaction rate (A+B->C) distribution in the double injection reactor according to different TKI models coupled with the $\kappa - \epsilon$ turbulence model. Aspect ratio modified for the sake of readability.

3.2.2. Tubular reactor with static mixer

The isothermal tubular reactor equipped with a static mixer to provide a fast mixing between reactants A and B, as sketched in Figure 14, was used as a second case study.

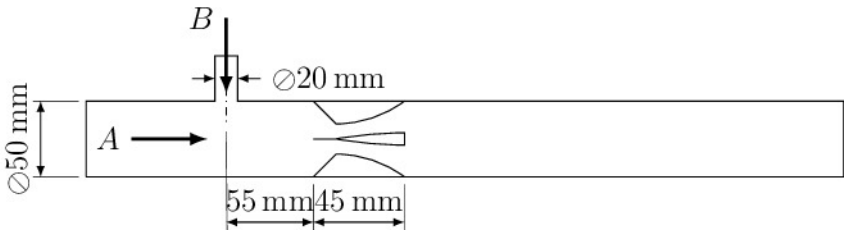

Figure 14 Tubular reactor with static mixer geometry.

The following reaction occurs

$$A + B \rightarrow C + H_2O \qquad r = \mathcal{K} c_A c_B \#(24)$$

with $\mathcal{K} = 0.4E-3 \div 50\, m^3 kmol^{-1} s^{-1}$. Reactant A was fed from the reactor entrance, while the other reactant B from the side inlet. Boundary conditions used for the simulations are shown in Table 5.

After a mesh independence analysis, the number of cells used in all the computations was equal to about 470,000.

The effect of changing the Da value from Da<<1 to Da>>1 was investigated by changing the value of the kinetic constant leading to Da values in the range $10^{-2} \div 10^{2}$.

Inlet A	$\omega_A = 0.1$ $v_A = 0.1 \frac{m}{s}$ $f = 1$ $\sigma_1^2 = \sigma_2^2 = \sigma_3^2 = 0$
Inlet B	$\omega_B = 0.1$ $v_B = 0.6 \frac{m}{s}$ $f = 0$ $\sigma_1^2 = \sigma_2^2 = \sigma_3^2 = 0$
Outlet	$Mixture\ fraction\ flux = 0$ $Variances\ flux = 0$
Wall	No slip condition

Table 5 Boundary conditions used for simulating the tubular reactor with static mixer

These values are sufficient to read the asymptotic behavior of the hybrid model, that should degenerate in the LR model for Da<<1 and to MTS model for Da >>1. In Figure 15 the results obtained using the different TKI models are reported in terms of conversion of reagent A as a function of Da for three different models.

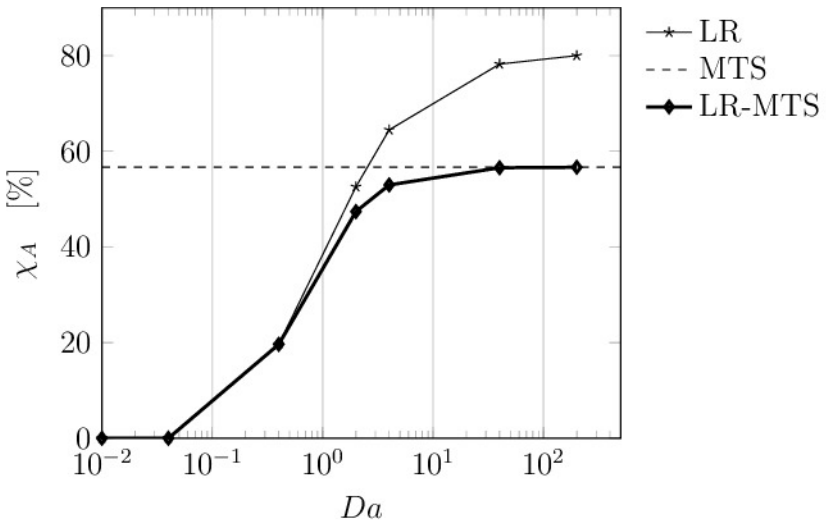

Figure 15 Reagent A conversion as a function of Da according to different TKI models coupled with the $\kappa - \epsilon$ turbulence model.

We can see that, as expected, the hybrid LR-MTS model results are always lower than these of the LR and MTS models. Moreover, for Da<<1 the LR-MTS hybrid model gives the same results as the LR model, while for Da>>1 the LR-MTS hybrid model results superimpose those of the MTS model.

However, in the transition region where neither Da<<1 nor Da>>1, the hybrid LR-MTS model provides results which are different from both the LR and MTS asymptotic models.

4. Conclusions

A new TKI model for liquid phase reactions, which combines the Laminar Rate model (for kinetic controlled systems) with the Multiple Time Scales model (for turbulence controlled systems), was proposed. The main feature of this model is that it can be used also when kinetic and turbulent mixing characteristic times are comparable, while the existing models can be used only in the limiting conditions of Da>>1 or Da<<1. Moreover, its simplicity allows it to be easily embedded in RANS-CFD codes in order to have reliable predictions in a reasonably short time, with rather low computational resources. It should be mentioned that very complex TKI models, such as the 5-peak beta pdf model, are less suitable for industrial applications, as they require large computational resources and suffer large uncertainties in the initial and boundary conditions.

A sensitivity analysis of the coupling between the turbulence model and the proposed TKI approach has been performed, showing that on the overall the $\kappa - \epsilon$ and Low Re models give the best results. Furthermore, two different case studies were investigated showing the correct qualitative performances of the proposed model in all the conditions investigated.

In conclusion, the proposed LR-MTS model can be considered an effective tool for liquid-phase reactions that can be adopted for every value of Da, therefore filling the gap of previously proposed TKI models, which can be used only in the limiting conditions of either Da>>1 or Da<<1.

References

[1] L. Rudniak, A. Milewska, E. Molga, CFD simulations for safety of chemical reactors and storage tanks, Chem. Eng. Technol. 34 (2011) 1781–1789. doi:10.1002/ceat.201100128.

[2] M. Rizzotto, F. Florit, R. Rota, V. Busini, Thermocouples positioning for early-warning detection of thermal runaway, Int. J. Adv. Sci. Eng. Technol. 6 (2018) 45–49. IRAJ DOI Number - IJASEAT-IRAJ-DOI-10887

[3] J.P. Torré, D.F. Fletcher, T. Lasuye, C. Xuereb, An experimental and CFD study of liquid jet injection into a partially baffled mixing vessel: A contribution to process safety by improving the quenching of runaway reactions, Chem. Eng. Sci. 63 (2008) 924–942. doi:10.1016/j.ces.2007.10.031.

[4] D. C. Wilcox, Turbulence modeling for CFD, Third edition, DCW Industries, 2006

[5] S. B. Pope, Turbulent Flows, Cambridge University Press, 2000

[6] B.F. Magnussen, B.H. Hjertager, On mathematical modeling of turbulent combustion with special emphasis on soot formation and combustion, Symp. Combust. 16 (1977) 719–729. doi:10.1016/S0082-0784(77)80366-4.

[7] B.F. Magnussen, On the structure of turbulence and a generalized eddy dissipation concept for chemical reaction in turbulent flow, 19th Am. Inst. Aeronaut. Astronaut. Aerosp. Sci. Meet. (1981) 1–6. doi:10.2514/6.1981-42.

[8] ANSYS Inc., ANSYS Fluent Theory Guide – release 16.2, 2015

[9] J. Baldyga, J.R. Bourne, A Fluid Mechanical Approach to Turbulent Mixing and Chemical Reaction Part Ii Micromixing in the Light of Turbulence Theory, Chem. Eng. Commun. 28 (1984) 243–258. doi:10.1080/00986448408940136.

[10] J. Baldyga, Turbulent mixer model with application to homogeneous, instantaneous chemical reactions, Chem. Eng. Sci. 44 (1989) 1175–1182. doi:10.1016/0009-2509(89)87016-2.

[11] B.E. Launder, D.B. Spalding, Mathematical models of turbulence, London: Academic Press, 1972

[12] R. O. Fox, The spectral relaxation model of the scalar dissipation rate in homogeneous turbulence, Phys. Fluids. 7 (1995) 1082-1094. doi:10.1063/1.868550.

[13] R.O. Fox, The Lagrangian spectral relaxation model of the scalar dissipation in homogeneous turbulence, Phys. Fluids. 9 (1997) 2364–2386. doi:10.1063/1.869357.

[14] R.O. Fox, On the relationship between Lagrangian micromixing models and computational fluid dynamics, Chem. Eng. Process. Process Intensif. 37 (1998) 521–535. doi:10.1016/S0255-2701(98)00059-2.

[15] L.K. Hjertager, B.H. Hjertager, T. Solberg, CFD modelling of fast chemical reactions in turbulent liquid flows, Comput. Chem. Eng. 26 (2002) 507–515. doi:10.1016/S0098-1354(01)00799-2.

[16] L. K. Hjertager, Experimental and computational study of mixing and fast chemical reactions in turbulent liquid flows, Ph.D. thesis, Esbjerg: Esbjerg Institute of Techonology, Aalborg University, 2004

[17] G.K. Batchelor, Small scale variation of convected quantities like temperature in a turbulent fluid, J. Fluid Mech. 5 (1959) 113.

[18] S. Subramaniam, S.B. Pope, Comparison of mixing model performance for nonpremixed turbulent reactive flow, Combust. Flame. 117 (1999) 732–754. doi:10.1016/S0010-2180(98)00135-7.

[19] L.K. Hjertager Osenbroch, B.H. Hjertager, T. Solberg, Experiments and CFD Modelling of Fast Chemical Reaction in Turbulent Liquid Flows, Int. J. Chem. React. Eng. 3 (2005). doi:10.2202/1542-6580.1251.

[20] S. Komori, K. Nagata, T. Kanzaki, Y. Murakami, Measurements of mass flux in a turbulent liquid flow with a chemical reaction, AIChE J. 39 (1993) 1611–1620. doi:10.1002/aic.690391005.

[21] J. W. Neudeck, Multi-peak presumed pdf simulation of turbulent reacting flows, M.Sc. Thesis, Kansas State University, 1999

[22] V. Zhdanov, A. Chorny, Development of macro- and micromixing in confined flows of reactive fluids, Int. J. Heat Mass Transf. 54 (2011) 3245–3255. doi:10.1016/j.ijheatmasstransfer.2011.04.006.

[23] W. B. DeMore, S. P. Sander, D. M. Golden, R. F. Hampson, M. J. Kurylo, C. J. Howard, A. R. Ravishankara, C. E. Kolb, M. J. Molina, Chemical kinetics and photochemical data for use in stratospheric modelling. Evaluation number 12, JPL Publication 97 (4), 1997, 1-266

[24] R. Pohorecki, J. Baldyga, New Model of Micromixing in Chemical Reactors . I . General Development and Application to a Tubular Reactor, Ind. Eng. Chem. Fundam. 22 (1983) 392–397.